THE AMERICAN SOCIETY OF MECHANICAL ENGINEERS
345 E. 47 St., New York, N.Y. 10017

91-GT-6

Generalized Polynomial Expansion Method for the Dynamic Analysis of Rotor-Bearing Systems

TING NUNG SHIAU and JON LI HWANG
Institute of Aeronautics and Astronautics
National Cheng Kung University
Tainan, Taiwan, R.O.C.

ABSTRACT

The determination of critical speeds and modes and the unbalance response of rotor-bearing systems is investigated with the application of a technique called the generalized polynomial expansion method (GPEM). This method can be applied to both linear and nonlinear rotor systems, however, only linear systems are addressed in this paper. Three examples including single spool and dual rotor systems are used to demonstrate the efficiency and the accuracy of this method. The results indicate a very good agreement between the present method and the finite element method (FEM). In addition, computing time will be saved using this method in comparison with the finite element method.

NOMENCLATURE

$a_n(t), b_m(t)$	: Generalized coordinates.
$A(x)$	: Cross sectional area of the shaft.
$c^b_{yyj}, c^b_{zzj}, c^b_{yzj}$	: Damping coefficients of the j-th bearing.
d	: Diameter of the shaft.
e^d_i	: Eccentricity of the i-th disc.
$e(x)$	: Eccentricity of the shaft at position x.
$E(x)$	: Elastic modulus of the shaft.
$I(x)$	: Cross sectional area moment.
I_D, I_P	: Diametral and polar mass moment of inertia of the shaft.
I^d_{Di}, I^d_{Pi}	: Diametral and polar mass moment of inertia of the i-th disc.
$k^b_{yyj}, k^b_{zzj}, k^b_{yzj}$	: Elastic constant of the j-th bearing.
ℓ	: Total length of the shaft.
m^d_i	: Mass of the i-th disc.
N_d	: Total number of the disc.
N_b	: Total number of the bearings.
N_p	: Total number of polynomials.
$\underline{Q}_f, \underline{Q}_b$	: Magnitude of steady state forward and backward response.
V^d_i, W^d_i	: Translational displacements of the i-th disc.
V^b_j, W^b_j	: Translational displacements of the j-th bearing.
α_r	: Real part of eigenvalues.
δ_r	: Log decrements.
λ	: Whirl ratio (Ω/ω).
$\rho(x)$	: Density of the shaft, mass/unit length.
Ω	: Rotating speed of the shaft.
ω	: Whirl speed.

INTRODUCTION

Various methods for the determination of critcal speeds and modes and the unbalance response of rotor-bearing systems have been developed and widely used during the past few decades. These methods may be categorized in two major classes. The first is the discretization method which ap-

Presented at the International Gas Turbine and Aeroengine Congress and Exposition
Orlando, FL June 3-6, 1991

proximates a rotor system using a finite number of degrees-of-freedom. In this case, the equations of motions are a set of ordinary differential equations. This category can also be divided into two techniques. One is the state vector-transfer matrix method (Myklestad, 1944; Prohl, 1945; Lund, 1967, 1974a, 1974b). The other is the direct stiffness method (Ruhl and Booker, 1972; Dimaragonas, 1975; Gasch, 1976; Nelson and McVaugh, 1976; Childs, 1978; Nelson, 1980; Adams, 1980; Childs and Graviss, 1982). These techniques have been successfully utilized to analyze the dynamic characteristics of rotor systems. The second is the analytical method (Gladwell and Bishop, 1959; Dimentberg, 1961; Eshleman and Eubanks, 1969; Lee and Jei, 1988) which treats the rotor systems as distributed parameter system with a set of partial differential equations describing the system motion.

At the present time, the state vector-transfer matrix method is limited to linear frequency domain analysis and the direct stiffness method may be the only validated tool available for both linear and nonlinear time domain analysis. However, the use of the direct stiffness method may lead to high computation time and costs for large rotor systems. Kumar and Sankar (1986) proposed a new transfer matrix method for response analysis of large dynamic systems. Gu (1986) introduced an improved transfer matrix-direct integration method to determine the critical speeds and unbalance response. A method which combines the methodologies of finite elements and transfer matrix, has been applied (Subbiah et al., 1988) for the transient dynamic analysis of rotors. In addition, Crandall and Yeh (1986, 1989) proposed a modelling approach for the multi-rotor system. It generates the internal modes of each rotor component without solving the eigenvalue problems. And each mode of the rotating shaft is represented by fourth order polynomials with piecewise constant coefficients. It is noted that for the finite element method (FEM) the deformation of a rotating shaft using a typical beam element is described by third order polynomials with piecewise constant coefficients. Also, these coefficients are expressed as functions of the deflections at node points.

In this paper, the analysis method introduced by Shiau and Hwang (1989), has been modified and is called the generalized polynomial expansion method (GPEM). The method approximates the displacements of an entire rotating shaft in the global assumed modes sense with (N_p-1)-th order polynomials with time dependent coefficients. This is different from the finite element method in a subdomain sense and from the modelling approach proposed by Crandall and Yeh (1986,1989). The present approach can be applied to both linear and nonlinear rotor-bearing systems. The application of the GPEM to nonlinear systems has been investigated and submitted for publication [Hwang and Shiau (1989)]. The efficiency and the accuracy of using this method will be demonstrated through examples. The critical speeds, mode shapes, and unbalance response of the examples are shown in this study.

EQUATIONS FORMULATION

The basic configuration of a rotor-bearing system usually consists of the components: rigid discs, flexible shafts, and bearings, such as shown in Figure 1. The lateral displacements and the rotor eccentricity due to mass unbalance are assumed to be small. To describe the system motion, two reference frames are utilized. One is a fixed reference X-Y-Z and the other is a rotating reference x-y-z. The X and x axes are collinear and coincident with the undeformed bearing centerline. The two reference frames have a single rotation ωt difference about X with ω denoting a whirl speed.

It is assumed that all the deflections and forces are parallel to the Y-Z plane. The deflection of a cross-section of shaft consists of two translations (V,W) and two rotations (B,Γ). It is assumed that the deflections can be expressed as functions of position along the rotating axis x and time t, i.e.

$$\begin{aligned} V = V(x,t) \quad &, \quad W = W(x,t) \\ B = B(x,t) \quad &, \quad \Gamma = \Gamma(x,t) \end{aligned} \tag{1}$$

The rotations(B,Γ) are related to the translations (V,W) by the equations

$$\begin{aligned} B(x,t) &= -\frac{\partial W(x,t)}{\partial x} \\ \Gamma(x,t) &= \frac{\partial V(x.t)}{\partial x} \end{aligned} \tag{2}$$

To derive the equations of motion, the Lagrangian approach is employed. This requires the calculation of the kinetic and potential energies of the system. The kinetic and potential energies of the system can be expressed in terms of the displacements and their derivatives. The total kinetic energy (T) and the potential energy (U) of the system can be expressed as

$$T = T_s + T_d + T_e \tag{3}$$

$$U = U_s + U_b \tag{4}$$

where T_s and T_d are the kinetic energy of the shaft and the disc; T_e is the kinetic energy related to the eccentricity; U_s and U_b are the strain energy of the shaft and bearings. They are of the forms:

$$\begin{aligned} T_s =& \frac{1}{2}\int_0^\ell \rho A(\dot{V}^2 + \dot{W}^2)dx + \frac{1}{2}\int_0^\ell I_D(\dot{B}^2 + \dot{\Gamma}^2)dx \\ &+ \frac{1}{2}\Omega\int_0^\ell I_P(\Gamma\dot{B} - B\dot{\Gamma})dx + \frac{1}{2}\Omega^2\int_0^\ell I_p dx \end{aligned} \tag{5}$$

$$\begin{aligned} T_d =& \sum_{i=1}^{N_d}\{\frac{1}{2}m_i^d(\dot{V}_i^2 + \dot{W}_i^2) \\ &+ \frac{1}{2}I_{Di}^d(\dot{B}_i^2 + \dot{\Gamma}_i^2) + \frac{1}{2}\Omega I_{pi}^d(\dot{B}\Gamma - \dot{\Gamma}B) \\ &+ \frac{1}{2}\Omega^2 I_{pi}^d\} \end{aligned} \tag{6}$$

$$T_e = \int_0^\ell e(x)\rho(x)A(x)\Omega[-\dot{V}\sin(\Omega t + \phi) + \dot{W}\cos(\Omega t + \phi)]dx$$

$$+\int_0^\ell e^2(x)\rho(x)A(x)\Omega^2 dx + \sum_{i=1}^{N_d}\Big\{e_i^d\Omega m_i^d[-\dot V_i \sin(\Omega t + \phi_i^d) + \dot W_i \cos(\Omega t + \phi_i^d)] + m_i^d(e_i^d)^2\Omega^2\Big\} \quad (7)$$

$$U_s = \frac{1}{2}\int_0^\ell EI[(V'')^2 + (W'')^2]dx \quad (8)$$

$$U_b = \sum_{j=1}^{N_b}\{\frac{1}{2}K_{yyj}^b V_j^2 + \frac{1}{2}K_{zzj}^b W_j^2 + K_{yzj}^b V_j W_j\} \quad (9)$$

The dissipation function (F) due to bearing damping is given by

$$F = \sum_{j=1}^{N_b}[\frac{1}{2}C_{yyj}^b(\dot V_j^b)^2 + \frac{1}{2}C_{zzj}^b(\dot W_j^b)^2 + C_{yzj}^b \dot V_j^b \dot W_j^b] \quad (10)$$

The denotation of parameters involved in equations (5)-(10) are given in the Nomenclature.

The assumed modes technique for the undamped rotor-bearing systems, proposed by Shiau and Hwang (1989), has been generalized for damped systems using the following displacement functions:

$$V(x,t) = \sum_{n=1}^{N_p} a_n(t)x^{n-1}$$
$$W(x,t) = \sum_{m=1}^{N_p} b_m(t)x^{m-1} \quad (11)$$

where the $a_n(t)$ and $b_m(t)$ are generalized coordinates. The corresponding rotational displacements, using equation (2), are given by

$$\Gamma(x,t) = \frac{\partial V(x,t)}{\partial x} = \sum_{n=2}^{N_p}(n-1)x^{n-2}a_n(t)$$
$$B(x,t) = \frac{-\partial W(x,t)}{\partial x} = -\sum_{m=2}^{N_p}(m-1)x^{m-2}b_m(t) \quad (12)$$

where the integer N_p is the number of polynomials. As noted in Shiau and Hwang (1989), the first two terms of the polynomial expansion of equation (11) must exist i.e. the associated coefficients a_1, a_2, b_1, b_2 can not be zero. The constant term, the first two terms, and the first three terms of the expansion represent a cylindrical mode, conical mode, and bending mode, respectively. Moreover, if rigid body modes exist in the system, the first two terms will be dominant. It should be noted that other types of polynomials may be used as candidates for this method. Trigonometric polynomials have been used with minimal success and other choices are under investigation. The present method is also applicable to those systems with geometric displacement constraints. The additional requirement is to impose the required constraint or constraints. This will be shown in the first example of single uniform shaft.

Substituting equations (11) and (12) and their derivatives into equations (5)-(10), gives the total kinetic energy, potential energy, and dissipation energy in terms of time dependent polynomial coefficients (a_n, b_m) and their corresponding derivatives ($\dot a_n, \dot b_m$). To find the equations of motion governing the rotor-bearing system, the Lagrangian approach is applied i.e.

$$\frac{d}{dt}[\frac{\partial}{\partial \dot q_i}(T-U)] - \frac{\partial}{\partial q_i}(T-U) + \frac{\partial F}{\partial \dot q_i} = 0 \quad (13)$$

where the generalized coordinates q_i are the a_n and b_m with $n, m = 1, N_p$. For constant rotating speed, the equations of motion may be expressed as follows:

$$\begin{bmatrix} M & O \\ O & M \end{bmatrix}\begin{Bmatrix} \ddot{\underline{a}} \\ \ddot{\underline{b}} \end{Bmatrix} + \Omega\begin{bmatrix} O & G \\ -G & O \end{bmatrix}\begin{Bmatrix} \dot{\underline{a}} \\ \dot{\underline{b}} \end{Bmatrix} + \begin{bmatrix} C_{yy} & C_{yz} \\ C_{zy} & C_{zz} \end{bmatrix}\begin{Bmatrix} \dot{\underline{a}} \\ \dot{\underline{b}} \end{Bmatrix} + \begin{bmatrix} K_s & O \\ O & K_s \end{bmatrix}\begin{Bmatrix} \underline{a} \\ \underline{b} \end{Bmatrix} + \begin{bmatrix} K_{yy} & K_{yz} \\ K_{zy} & K_{zz} \end{bmatrix}\begin{Bmatrix} \underline{a} \\ \underline{b} \end{Bmatrix} = \begin{Bmatrix} \underline{R}_a \\ \underline{R}_b \end{Bmatrix} \quad (14)$$

where the coefficient vectors $\underline{a}$ and $\underline{b}$ are

$$\underline{a} = \{a_1, \ldots, a_{N_p}\}^T$$
$$\underline{b} = \{b_1, \ldots, b_{N_p}\}^T \quad (15a)$$

and the $N_p \times N_p$ component matrices, $M, G, C_{yy}, C_{yz}, C_{zz}, K_s, K_{yy}, K_{yz}$, and K_{zz} are shown in Appendix A. The $N_p \times 1$, forcing vectors, $\underline{R}_a$ and $\underline{R}_b$ are

$$\underline{R}_a = \{R_{a1}\ R_{a2}\ \ldots\ R_{aN_p}\}^T$$
$$\underline{R}_b = \{R_{b1}\ R_{b2}\ \ldots\ R_{bN_p}\}^T \quad (15b)$$

where

$$R_{aj} = \int_0^\ell e(x)\rho(x)A(x)\Omega^2\cos(\Omega t + \phi)x^{j-1}dx + \sum_{i=1}^{N_d} e_i^d m_i^d \Omega^2 \cos(\Omega t + \phi_i)x_i^{j-1} \quad (15c)$$

$$R_{bj} = \int_0^\ell e(x)\rho(x)A(x)\Omega^2\sin(\Omega t + \phi)x^{j-1}dx + \sum_{i=1}^{N_d} e_i^d m_i^d \Omega^2 \sin(\Omega t + \phi_i)x_i^{j-1}$$

In this work, the shaft eccentricity is considered to be negligible. Then the first term of the expressions R_{aj} and R_{bj}, shown in equation (15c), vanishes. In addition, the $N_p \times N_p$ damping and stiffness matrices, C_{yz} and K_{yz}, are considered as symmetric i.e. $C_{yz} = C_{zy}$ and $K_{yz} = K_{zy}$.

For the simplicity and convenience, the $N_p \times 1$ complex vector $\underline{p}$ and its conjugate $\tilde{\underline{p}}$ are introduced,

$$\underline{p} = \underline{a} + i\underline{b}$$
$$\tilde{\underline{p}} = \underline{a} - i\underline{b} \quad (16)$$

and equation (14) can then be rewritten as:

$$[M]\ddot{\underline{p}} + ([C_1] - i\Omega[G])\dot{\underline{p}} + ([C_2] + i[C_{yz}])\dot{\tilde{\underline{p}}} + ([K_s] + [K_1])\underline{p} + ([K_2] + i[K_{yz}])\tilde{\underline{p}}$$

$$= \sum_{j=1}^{N_d} e_j^d m_j^d \Omega^2 \underline{R}_j^d e^{i(\Omega t + \phi_j^d)} \quad (17)$$

where the $N_p \times N_p$ matrices $[K_1]$,$[K_2]$,$[C_1]$, and $[C_2]$ are all real and symmetric matrices and of the form

$$[K_1] = \frac{1}{2}([K_{yy} + [K_{zz}]), \quad [K_2] = \frac{1}{2}([K_{yy}] - [K_{zz}])$$
$$[C_1] = \frac{1}{2}([C_{yy}] + [C_{zz}]), \quad [C_2] = \frac{1}{2}([C_{yy}] - [C_{zz}]) \quad (18a)$$

and the force vector $\underline{R}_j^d$ is defined by

$$\underline{R}_j^d = \left\{ R_{j1}^d \ R_{j2}^d \ \ldots \ R_{jN_p}^d \right\}^T$$
$$R_{jk}^d = x_j^{k-1}\ , \quad k = 1, N_p \quad (18b)$$

CRITICAL SPEEDS AND STEADY STATE UNBALANCE RESPONSE

Critical Speeds

The critical speed of the damped system governed by equation (17) is calculated using the homogeneous form. Assume the homogeneous solution of equation (17) to be of the form

$$\underline{p} = \underline{R}_f e^{i\omega t} + \underline{R}_b e^{-i\omega t} \quad (19)$$

where ω is the natural frequency or the whirl speed of the system and substitute equation (19) into the homogeneous form of equation (17), to obtain the following equations

$$(-\omega^2[M] + \omega\Omega[G] + [K_3] + i\omega[C_1])\underline{R}_f +$$
$$([K_2] - \omega[C_{yz}] + i[K_{yz}] + i\omega[C_2])\tilde{\underline{R}}_b = 0 \quad (20a)$$
$$(-\omega^2[M] - \omega\Omega[G] + [K_3] - i\omega[C_1])\underline{R}_b$$
$$+ ([K_2] + \omega[C_{yz}] + i[K_{yz}] - i\omega[C_2])\tilde{\underline{R}}_f = 0 \quad (20b)$$

where $[K_3] = [K_s] + [K_1]$. For undamped orthotropic systems, one can calculate the critical speeds by taking the conjugate of equation (20b) and combining with equation (20a) to obtain

$$\left(\begin{bmatrix} [K_3] & [K_2] + i[K_{yz}] \\ [K_2] - i[K_{yz}] & [K_3] \end{bmatrix} - \omega^2 \begin{bmatrix} [M] - \lambda[G] & 0 \\ 0 & [M] + \lambda[G] \end{bmatrix} \right) \begin{Bmatrix} \underline{R}_f \\ \tilde{\underline{R}}_b \end{Bmatrix} = \{0\} \quad (21)$$

where $\lambda = \frac{\Omega}{\omega}$ is the spin/whirl ratio. Setting λ to a specified value and solving the eigenvalue problem governed by equation (21), provides the critical speeds of the rotor bearing system. The whirl speeds can also be obtained by rewriting equation (14) in the first order form

$$\begin{bmatrix} [M] & 0 & 0 & 0 \\ 0 & [M] & 0 & 0 \\ 0 & 0 & [I] & 0 \\ 0 & 0 & 0 & [I] \end{bmatrix} \begin{Bmatrix} \ddot{\underline{a}} \\ \ddot{\underline{b}} \\ \dot{\underline{a}} \\ \dot{\underline{b}} \end{Bmatrix} +$$

$$\begin{bmatrix} [C_{yy}] & [C_{yz}] + \Omega[G] & [K_s] + [K_{yy}] & [K_{yz}] \\ [C_{zy}] - \Omega[G] & [C_{zz}] & [K_{zy}] & [K_s] + [K_{zz}] \\ -[I] & 0 & 0 & 0 \\ 0 & -[I] & 0 & 0 \end{bmatrix}$$
$$\begin{Bmatrix} \dot{\underline{a}} \\ \dot{\underline{b}} \\ \underline{a} \\ \underline{b} \end{Bmatrix} = \{0\} \quad (22)$$

and directly solving equation (22) for specified rotation speeds.

Steady State Unbalance Response

The steady state unbalance response of the system governed by equation (17) can be assumed of the form

$$\underline{p} = \underline{Q}_f e^{i\Omega t} + \underline{Q}_b e^{-i\Omega t} \quad (23)$$

where $\underline{Q}_f$ and $\underline{Q}_b$ are complex vectors which describe the amplitude and phase of forward and backward circular motion, respectively. Substituting equation (23) into equation (17), gives

$$[A_1]\underline{Q}_f + [B_1]\tilde{\underline{Q}}_b = \sum_{j=1}^{N_d} e_j^d m_j^d \Omega^2 \underline{R}_j^d e^{i\phi_j^d} \quad (24a)$$

$$[A_2]\underline{Q}_b + [B_2]\tilde{\underline{Q}}_f = \underline{0} \quad (24b)$$

where the $N_p \times N_p$ matrices $[A_1]$, $[A_2]$,$[B_1]$, and $[B_2]$ are of the form

$$[A_1] = -\Omega^2[M] + \Omega^2[G] + [K_s] + [K_1] + i\Omega[C_1]$$
$$[A_2] = -\Omega^2[M] - \Omega^2[G] + [K_s] + [K_1] - i\Omega[C_1]$$
$$[B_1] = [K_2] - \Omega[C_{yz}] + i([K_{yz}] + \Omega[C_1])$$
$$[B_2] = [K_2] + \Omega[C_{yz}] + i([K_{yz}] - \Omega[C_2]) \quad (25)$$

Solving for $\tilde{\underline{Q}}_b$ from equation (24b) in terms of $\underline{Q}_f$ and substituting into equation (24a), one obtains

$$\underline{Q}_f = \sum_{j=1}^{N_d} e_j^d m_j^d \Omega^2 ([A_1] - [B_1][\tilde{T}])^{-1} \underline{R}_j^d e^{i\phi_j^d} \quad (26)$$

where the $N_p \times N_p$ matrix $[\tilde{T}]$ is the conjugate of

$$[T] = [A_2]^{-1}[B_2] \quad (27)$$

The backward component of steady state unbalance response can be obtained by substituting equation (26) into equation (24b) and solving for $\underline{Q}_b$.

NUMERICAL EXAMPLES AND RESULTS

Three rotor-bearing systems are used to illustrate the accuracy and the efficiency of the generalized polynomial expansion method (GPEM). The first is a single uniform shaft supported by identical bearings with internal damping. The second is a multi-stepped rotor system with orthotropic bearings. Finally, a dual rotor system with intershaft bearing is considered.

The results for the three examples are presented in tabular and graphical form for various numbers of polynomial terms.

Single Uniform Shaft

A simply supported steel shaft studied by Lund (1974a) and Glasgow and Nelson (1979), is used as a basic example to examine the accuracy and the efficiency of the present method. Firstly, the shaft with two rigid simple supports at two ends is considered. The exact solution for whirl speeds can be derived as

$$\omega = \sqrt{\left(\frac{EI}{\rho A \ell^4}\right) \frac{(n\pi)^4}{1 + (n\pi)^2 \frac{I}{A\ell^2}(1 - 2\lambda)}} \ , \ n = 1, 2, \cdots \tag{28}$$

where all the parameters are defined in the Nomenclature. Before applying the present method, it is noted that the choices of the assumed modes for translational deformations in equation (11) are arbitrary, and equations (14) and (21) can be applied to a rotor system with no geometrical constraints. However, geometric constraints are introduced to this example as follows:

$$[B]\underline{a} = \underline{0} \quad \text{and} \quad [B]\underline{b} = \underline{0} \tag{29}$$

where the matrix $[B]$ is of the form

$$[B] = \begin{bmatrix} 1 & (x_1^b) & (x_1^b)^2 & \cdots & (x_1^b)^{N_p-1} \\ 1 & (x_2^b) & (x_2^b)^2 & \cdots & (x_2^b)^{N_p-1} \end{bmatrix} \tag{30}$$

with x_1^b and x_2^b denote the axial positions of the two supports. Then, one can obtain the following expressions

$$\underline{a} = \begin{bmatrix} R \\ I \end{bmatrix} \underline{a}_I \quad , \quad \underline{b} = \begin{bmatrix} R \\ I \end{bmatrix} \underline{b}_I \tag{31}$$

where

$$[R] = -\begin{bmatrix} 1 & x_1^b \\ 1 & x_2^b \end{bmatrix}^{-1} \begin{bmatrix} (x_1^b)^2 & (x_1^b)^3 & \cdots & (x_1^b)^{N_p-1} \\ (x_2^b)^2 & (x_2^b)^3 & \cdots & (x_2^b)^{N_p-1} \end{bmatrix} \tag{32}$$

and

$$\begin{aligned} \underline{a}_I^T &= \{a_3 \ a_4 \ \cdots, a_{N_p}\} \\ \underline{b}_I^T &= \{b_3 \ b_4 \ \cdots, b_{N_p}\} \end{aligned} \tag{33}$$

Substituting equation (31) into equation (14) and premultiplying equation (14) with the transpose of the transformation matrix $[R \ I]^T$ in equation (31), the governing equations of a rotor system with geometrical requirements are obtained. The following numerical results are obtained for the parameter value $I/A\ell^2 = 1/64$. Tables 1 and 2 show the comparison of whirl speeds obtained by present method, FEM, and the exact solution from equation (28) with whirl ratio $\lambda = -1$ and 1, respectively. It should be noted that the FEM employed in this study deals with the same energy contribution as in GPEM. In addition, the same eigensolver, EIGZS (IMSL, 1984), is applied for the calculation of whirl speeds for both methods. The results indicate that with the same degrees of freedom, the whirl speeds obtained by the present method are always more accurate than those obtained by the FEM.

Secondly, the two supports are considered to be identical flexible bearings. The stiffness coefficients of the bearings are $K_{yy} = K_{zz} = 1.7513 \times 10^7$ N/m, $K_{yz} = K_{zy} = -2.917 \times 10^6 N/m$ and the damping coefficients are $C_{yy} = C_{zz} = 1.752 \times 10^3 N \cdot s/m$ and $C_{yz} = C_{zy} = 0.0 N \cdot s/m$. The shaft is of diameter d=10.16 cm and length ℓ=127 cm. Consider the eigenvalues of equation (22) to be $\sigma_r = \alpha_r \pm i\omega_r$ and the log decrements δ_r of the damped precessional modes to be defined by

$$\delta_r = \frac{-2\pi\alpha_r}{\omega_r} \tag{34}$$

The density and the elastic modulus are $\rho = 0.7833 \times 10^4 Kg/m^3$ and $E = 0.2608 \times 10^{12} N/m^2$ respectively. The results of the log decrements (δ_r), the whirl speeds (ω_r), and the CPU time on a VAX 785 at a rotation speed of $\Omega = 400.0$ rad/sec are shown in Table 3 for the present method and in Table 4 for the finite element method (FEM). It should be noted that the CPU time calculated is based on the same eigensolver, EIGZF (IMSL, 1984). The results indicate that the convergence is very fast using GPEM. A comparison of whirl speeds using GPEM and FEM is shown in Figure 2. It shows a very good agreement between using GPEM and FEM. However the results shown in Tables 1-4 indicate that it is computationally more efficiency to use the GPEM. Figures 3-4 show the undamped eigen-modes of the system for Ω =1000.0, 5000.0 rad/sec respectively. Each shows four modes with forward (clockwise) motion and backward (counterclockwise) motion at certain rotation speed. The results show that the gyroscopic effect will increase when the rotation speed is increased and the motion will tend to be circular motion if the rotation speed is very large.

Multi – Stepped Rotor System

The rotor bearing system studied by Nelson and McVaugh (1976), is used to illustrate the merits of the pressent method for the determination of whirl speeds and unbalance response. The configuration of the rotor system and the corresponding data are shown in Figure 5 and Table 5 respectively. Tables 6 and 7 show the undamped whirl speeds using FEM and GPEM, and the log decrements and damped whirl speeds using FEM and GPEM, respectively. The whirl map for these methods is given in Figure 6. The results for FEM are obtained from a model with 18 elements and for GPEM are obtained from 17 polynomial terms. They show that the percentage of difference for the whirl speed is smaller than 6%. However the values of CPU time required is quite different. This indicates that considerable computing time can be saved using GPEM instead of FEM.

Figures 7–8 show the first three undamped eigen-modes for the rotation speed $\Omega = 1000.0, 5000.0$ rad/sec respectively. The results indicate that the increase of rotating speed will significantly influence the second mode. The undamped and damped steady state unbalance response are shown in Figures 9 and 10 with unit mass unbalance at the disc location, i.e. $e = 1$, respectively. The results indicate that for rotation speeds away from the critical speeds, the steady state responses are approximately the same for both undamped and damped cases. Also, when the rotation speed is large, the steady state response tends to be in forward synchronous circular motion.

Dual Rotor System

This example considers a dual rotor system with system parameters as shown in Figure 11 (Rajan, et al., 1985). The inner shaft with rotating speed Ω_1 is denoted by Rotor 1, and the outer shaft with rotating speed $\Omega_2 = 1.5\Omega_1$ is denoted by Rotor 2. Where the bearing supports are considered as isotropic and undamped with stiffness coefficients values $26.2795 \times 10^6\ N/m$ for station 1-0, $17.519 \times 10^6\ N/m$ for stations 6-0 and 7-0, and $8.7598 \times 10^6\ N/m$ for station 4-10. The motion of the dual rotor system is modelled by present method with $N_{p(1)} = 12$ for Rotor 1 and $N_{p(2)} = 8$ for Rotor 2. Moreover, each shaft can be treated as a substructure and the boundary coordinates are defined as the coordinates at bearing positions. The system equations of motion can be obtained by assembling the equations of each component. Table 8 shows the whirl speed results for various levels of modal trunction for $\Omega_1 = 1500.0\,rad/sec$. Figure 12 shows the whirl speed map. The results indicate that the first few forward and backward modes can be predicted with high accuracy even with high levels of modal truncation.

Based on present analysis and numerical results, the following remarks can be made:

(1) The equations of motion of a rotor system modelled by the present method generally require no geometric constraints. For some problems, it is necessary to satisfy the geometric boundary conditions. In these case, equation (29) can be introduced to describe the geometric constraints.

(2) Numerical instability may occurs when a large number of polynomial terms is chosen. To avoid the numerical instability, a similarity transformation can be applied to eliminate the scale of the difference between the elements in system matrices before solving the eigenvalue problem.

(3) Other types of functions may be chosen as the assumed modes, however, the generalized polynomials appear to be the most convenient and yield accurate solutions.

CONCLUSIONS

Three rotor-bearing systems including a single spool rotor and multi-shaft system have been studied to illustrate the merits of using the generalized polynomial expansion method (GPEM). The results for whirl speeds using the present method show considerable computing time savings for large rotor systems. The steady state unbalance response for the undamped and damped system is also studied and satisfactorily compared to those using the FEM. Moreover, the GPEM can be regarded as a global assumed modes method and can be applied to both linear and nonlinear rotor-bearing systems. The merits and procedures for using this method for analyzing nonlinear rotor-bearing systems have been investigated and are presented in a future paper.

ACKNOWLEGEMENT

The authors wish to thank Prof. Harold Nelson from Arizona State University, Tempe, AZ, for his valuable suggestion.

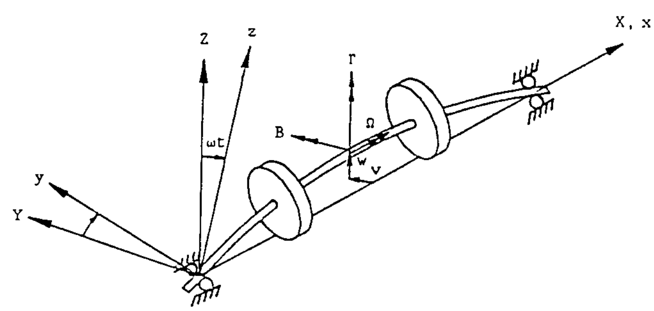

Figure 1 Typical rotor configuration and coordinates

Table 1 Comparison of whirl speeds of uniform shaft for $\lambda = -1$

$\dfrac{\textit{Whirl Speeds Obtained by GPEM}}{\textit{Whirl Speeds Obtained by FEM}}$ unit : $\sqrt{\dfrac{EI}{\rho A l^4}}$

DOF=2	4	6	8	12	16	Exa. Sol.
9.0389 / 9.0389	8.1631 / 8.1925	8.1608 / 8.1673	8.1608 / 8.1629	8.1608 / 8.1612	8.1608 / 8.1609	8.1608
29.135 / 29.135	23.473 / 25.842	23.383 / 23.645	23.383 / 23.472	23.383 / 23.401	23.383 / 23.389	23.383
	54.792 / 47.319	39.642 / 43.157	39.098 / 39.750	39.089 / 39.238	39.089 / 39.139	39.089
	85.615 / 67.403	56.250 / 62.403	54.539 / 60.118	54.478 / 55.078	54.478 / 54.684	54.478
		121.86 / 88.225	73.721 / 77.852	69.611 / 71.251	69.605 / 70.209	69.605
		163.71 / 104.42	92.454 / 101.96	84.591 / 93.276	84.561 / 85.967	84.561
			211.26 / 127.75	101.04 / 108.97	99.407 / 102.09	99.404
			264.57 / 140.89	117.38 / 130.62	114.19 / 125.92	114.17
				158.56 / 155.27	129.60 / 140.15	128.39
				184.26 / 181.44	145.01 / 160.49	143.56

† DOF = $N_p - 2$ for GPEM & DOF = $2 \times N_e$ for FEM.
‡ GPEM is the present method.

Table 2 Comparison of whirl speeds of uniform shaft for $\lambda = 1$

$\dfrac{\textit{Whirl Speeds Obtained by GPEM}}{\textit{Whirl Speeds Obtained by FEM}}$ unit : $\sqrt{\dfrac{EI}{\rho A l^4}}$

DOF=2	4	6	8	12	16	Exa. Sol.
11.926 / 11.926	10.735 / 10.771	10.732 / 10.740	10.732 / 10.735	10.732 / 10.732	10.732 / 10.732	10.732
85.621 / 85.621	64.233 / 71.554	63.780 / 64.615	63.779 / 64.049	63.779 / 63.832	63.779 / 63.796	63.779

† DOF = $N_p - 2$ for GPEM & DOF = $2 \times N_e$ for FEM.
‡ GPEM is the present method.

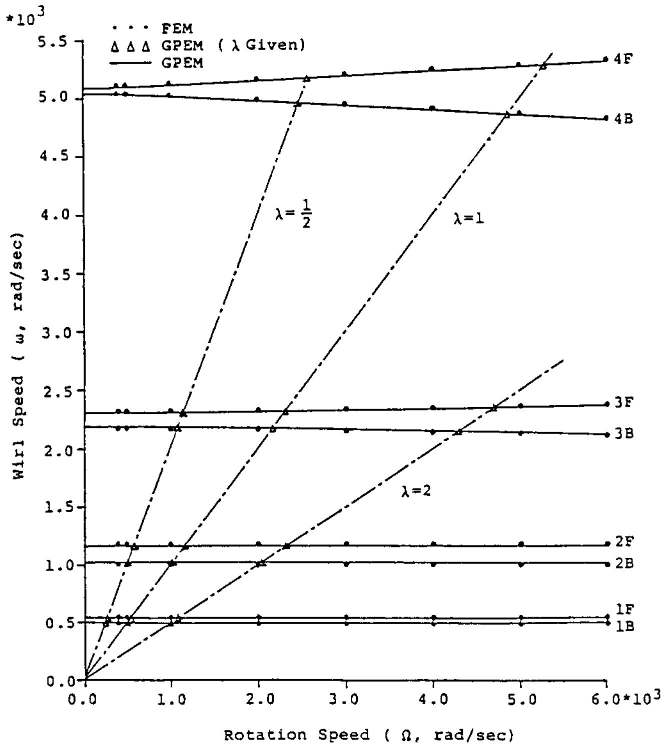

Figure 2 The whirl map using FEM and GPEM for unifrom rotor system

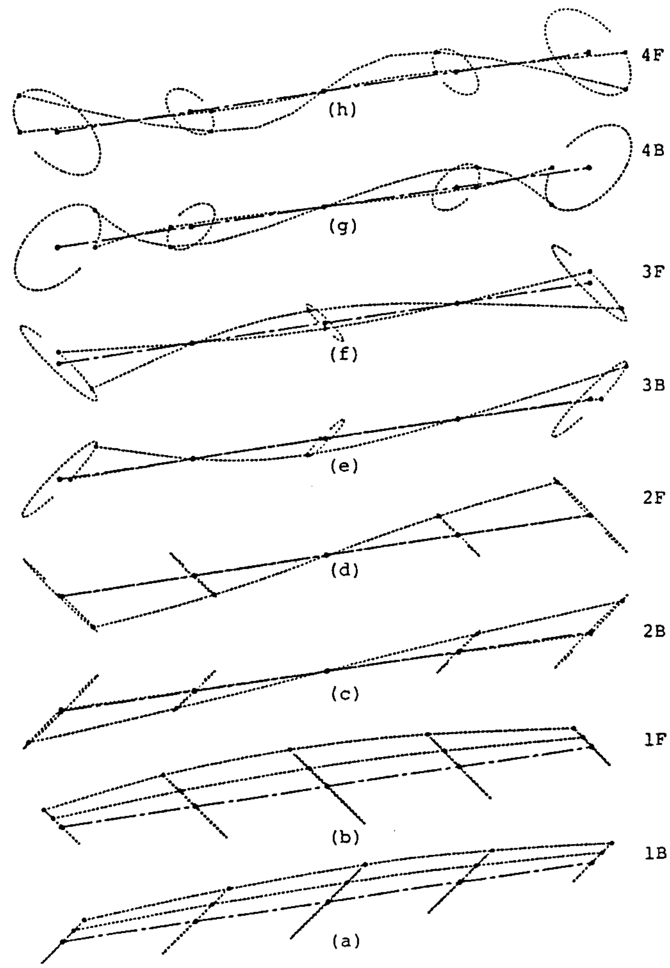

Figure 3 First four eigenmodes for rotation speed $\Omega = 1000.0$ rad/sec

Table 3 The results of log decrements, whirl speeds, and CPU time using GPEM for $\Omega = 400.0$ rad/sec

N_p	Log Decrements (δ_r), Whirl Speeds (ω_r), CPU Time (sec.)				
	Forward		Backward		CPU (sec.)
	δ_r	ω_r(rad/sec)	δ_r	ω_r(rad/sec)	
6	0.0853 0.2924 0.2683 0.1235	540.85 1160.7 2330.6 5245.3	0.1169 0.3479 0.2797 0.1224	497.05 1020.7 2209.2 5180.2	3.08
7	0.0852 0.2924 0.2577 0.1235	540.84 1160.7 2299.4 5245.3	0.1169 0.3479 0.2697 0.1224	497.04 1020.7 2182.5 5180.2	3.96
8	0.0852 0.2923 0.2577 0.1123	540.84 1160.6 2299.4 5087.8	0.1169 0.3479 0.2697 0.1114	497.04 1020.7 2182.5 5028.3	4.79
9	0.0852 0.2923 0.2577 0.1123	540.84 1160.6 2299.3 5087.8	0.1169 0.3479 0.2697 0.1114	497.04 1020.7 2182.5 5028.3	6.30

* N_p = Number of polynomials

Table 4 The results of log decrements, whirl speeds, and CPU time using FEM for $\Omega = 400.0$ rad/sec

N_e	Log Decrements (δ_r), Whirl Speeds (ω_r), CPU Time (sec.)				
	Forward		Backward		CPU (sec.)
	δ_r	ω_r(rad/sec)	δ_r	ω_r(rad/sec)	
2	0.0831 0.2951 0.2601 0.1071	545.86 1183.1 2318.6 5748.1	0.1214 0.3614 0.2738 0.1062	492.68 1010.4 2176.2 5681.2	3.28
3	0.0827 0.2881 0.2603 0.1113	544.98 1175.9 2321.4 5113.9	0.1209 0.3564 0.2744 0.1100	492.04 1006.1 2178.8 5046.4	5.35
4	0.0826 0.2892 0.2579 0.1143	544.83 1174.6 2315.0 5123.1	0.1208 0.3555 0.2723 0.1130	491.93 1005.3 2173.6 5053.9	8.02
5	0.0826 0.2879 0.2571 0.1134	544.79 1174.2 2312.7 5107.4	0.1208 0.3553 0.2715 0.1122	491.90 1005.0 2171.7 5038.7	12.23

* N_e = Number of elements

Table 5 Multi-stepped rotor configuration data

Element node no.	Node location (cm)	Bearing/ disk	Outer radius (cm)	Inner radius (cm)
1	-17.90		0.51	
2	-16.63		1.02	
3	-12.82		0.76	
4	-10.28		2.03	
5	-9.01	Disk No.1	2.03	
6	-7.74		3.30	
7	-7.23		3.30	1.52
8	-6.47		2.54	1.78
9	-5.20		2.54	
10	-4.44		1.27	
11	-1.39	Bearing No.1	1.27	
12	1.15		1.52	
13	4.96		1.52	
14	8.77		1.27	
15	10.80	Bearing No.2	1.27	
16	12.58		3.81	
17	13.60		2.03	
18	16.64		2.03	1.52
19	17.91			

Distributed rotor:

No.	Density (kg/m^3)	Elastic modulus (N/m^2)
1	7806	2.078×10^{11}

Disk:

No.	Location (cm)	Mass (kg)	Polar inertia (kg m^2)	Diametral inertia (kg m^2)
No.1	-9.01	1.401	0.0020	0.00136

Bearing:

No.	Location (cm)	$k_{yy} = k_{zz}$ (N/m)	$k_{yz} = k_{zy}$ (N/m)	$c_{yy} = c_{zz}$ (Ns/m)	$c_{yz} = c_{zy}$ (Ns/m)
No.1	-1.39	3.503×10^7	-8.756×10^6	1.752×10^3	0
No.2	10.08	3.503×10^7	-8.756×10^6	1.752×10^3	0

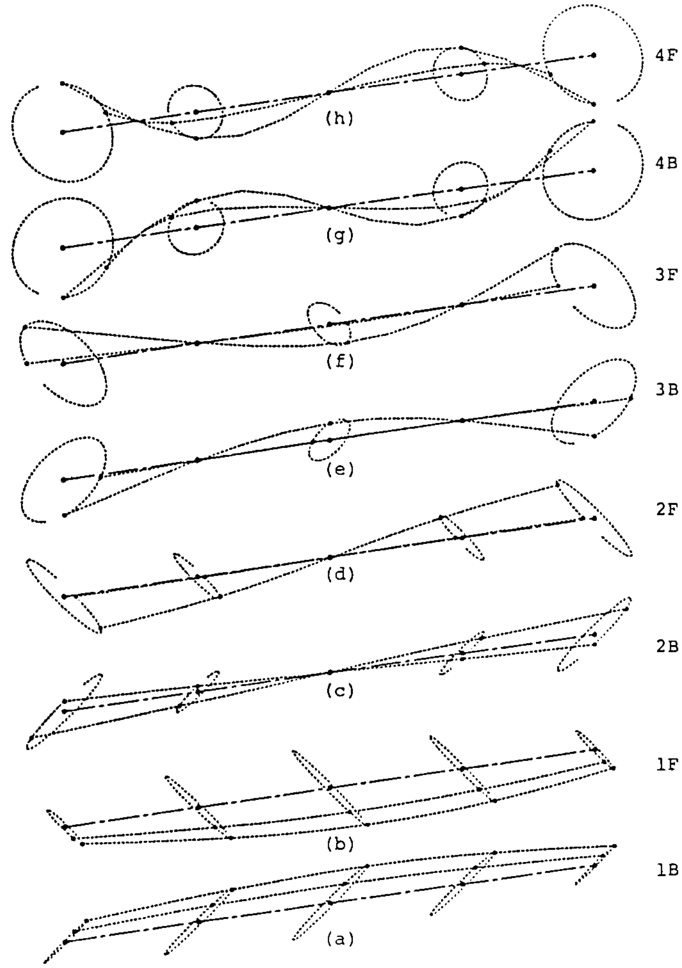

Figure 4 First four eigenmodes for rotation speed $\Omega = 5000.0$ rad/sec

Table 6 The whirl speeds and CPU time of undamped multi-stepped rotor system using FEM and GPEM

Undamped Whirl Speed (ω_r) / Rotating Speed (Ω)	GPEM		FEM	
	Forward	Backward	Forward	Backward
2000.0	1789.8 5160.8 8601.5	1488.1 4229.6 7245.0	1819.9 5026.2 8149.6	1541.1 4181.1 6833.9
3000.0	1816.5 5159.2 8784.4	1461.8 4227.2 7107.6	1852.6 5023.8 8314.1	1507.9 4176.5 6704.1
4000.0	1847.9 5156.8 8997.3	1430.9 4223.9 6957.9	1889.4 5020.2 8503.2	1470.4 4170.0 6562.6
5000.0	1882.1 5153.5 9229.2	1397.5 4219.6 6806.4	1928.0 5015.4 8705.3	1430.9 4161.6 6420.0
6000.0	1917.8 5149.1 9474.2	1362.7 4214.3 6658.3	1967.4 5008.9 8913.5	1390.6 4151.2 6281.9
CPU Time	58.65 (sec)		474.22 (sec)	

* The unit of Ω and ω_r is rad/sec.

Table 7 The log decrements and the damped whirl speed of multi-stepped rotor system using FEM and GPEM

Methods / Rotating Speed (Ω)	GPEM				FEM			
	Forward		Backward		Forward		Backward	
	δ_r	ω_r	δ_r	ω_r	δ_r	ω_r	δ_r	ω_r
2000	0.1327 0.4771 0.6227	1790.4 5166.2 8538.9	0.1972 0.7348 0.6736	1489.3 4227.8 7168.8	0.1169 0.4266 0.5956	1820.5 5034.3 8114.6	0.1609 0.6736 0.6833	1542.5 4187.6 6770.1
3000	0.1450 0.4778 0.6112	1817.0 5163.5 8722.4	0.1857 0.7320 0.6824	1463.0 4226.3 7032.0	0.1302 0.4299 0.5793	1853.3 5029.9 8281.8	0.1485 0.6686 0.6923	1509.3 4184.3 6641.1
4000	0.1568 0.4788 0.5986	1848.5 5159.6 8936.4	0.1747 0.7282 0.6914	1432.1 4224.0 6882.8	0.1422 0.4348 0.5603	1890.2 5023.5 8474.9	0.1378 0.6614 0.7011	1471.7 4179.6 6500.4
5000	0.1676 0.4803 0.5852	1882.7 5154.3 9169.8	0.1651 0.7231 0.7001	1398.6 4221.1 6732.0	0.1529 0.4416 0.5392	1928.9 5015.2 8681.9	0.1286 0.6522 0.7089	1432.0 4173.4 6358.9
6000	0.1776 0.4825 0.5714	1918.4 5147.4 9416.5	0.1564 0.7169 0.7083	1363.8 4217.5 6584.8	0.1628 0.4507 0.5165	1968.4 5004.6 8895.7	0.1207 0.6408 0.7151	1391.7 4165.5 6222.4
CPU Time	60.0 (sec)				500.0 (sec)			

* The unit of Ω and ω_r is rad/sec.

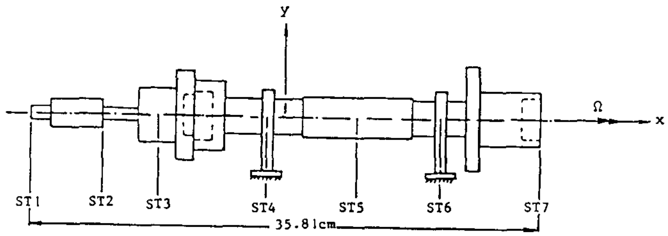

Figure 5 The configuration of multi-stepped rotor bearing system

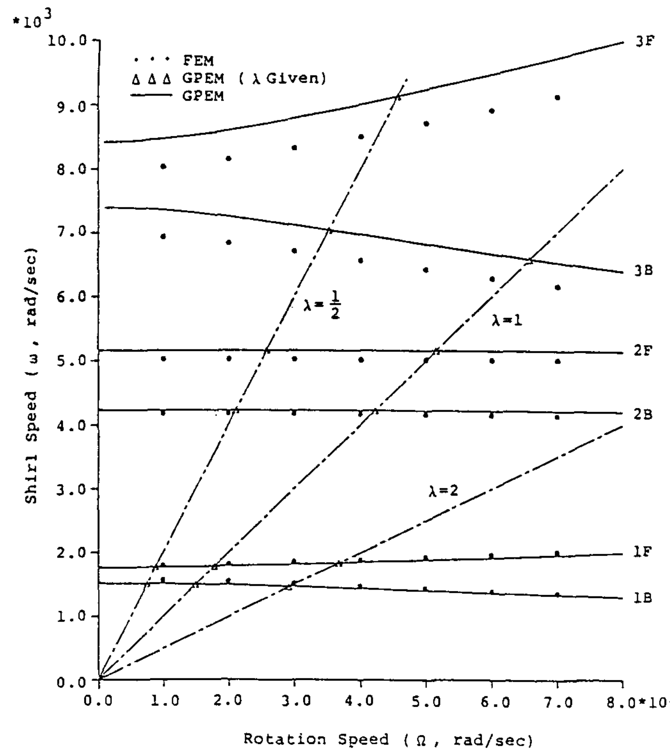

Figure 6 The whirl map using FEM and GPEM for multi-stepped rotor system

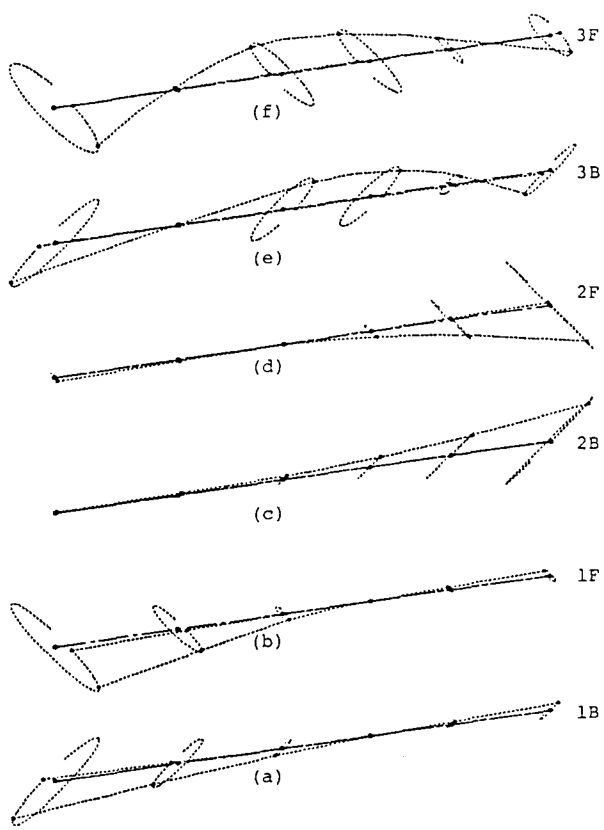

Figure 7 First three eigenmodes of multi-stepped rotor system for rotation speed $\Omega = 1000.0$ rad/sec

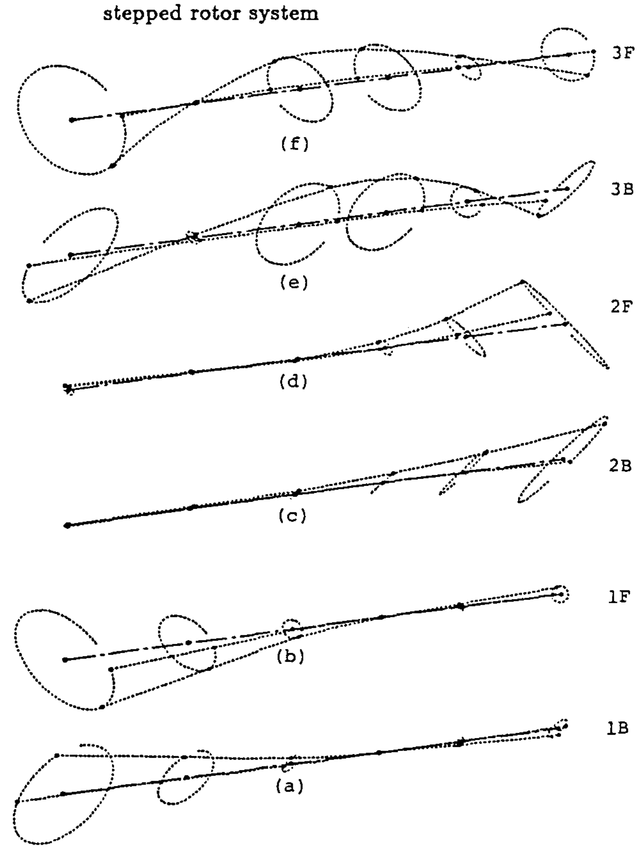

Figure 8 First three eigenmodes of multi-stepped rotor system for rotation speed $\Omega = 5000.0$ rad/sec

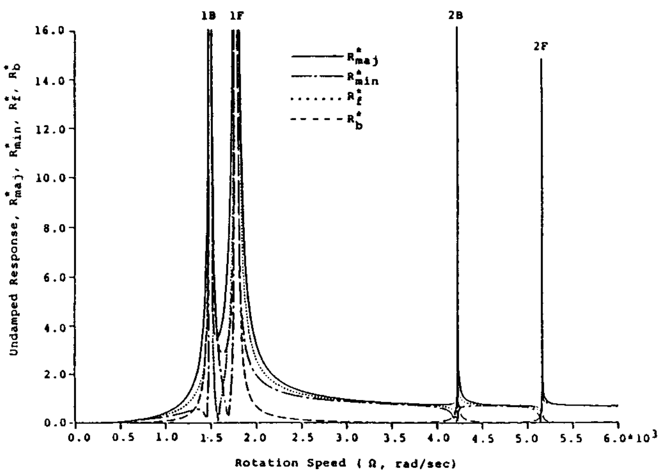

Figure 9 Undamped steady state unbalance response due to unit eccentricity

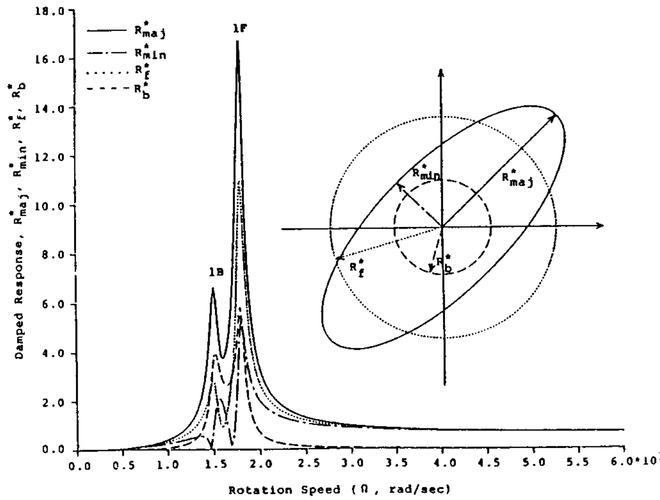

Figure 10 Damped steady state unbalance response due to unit eccentricity

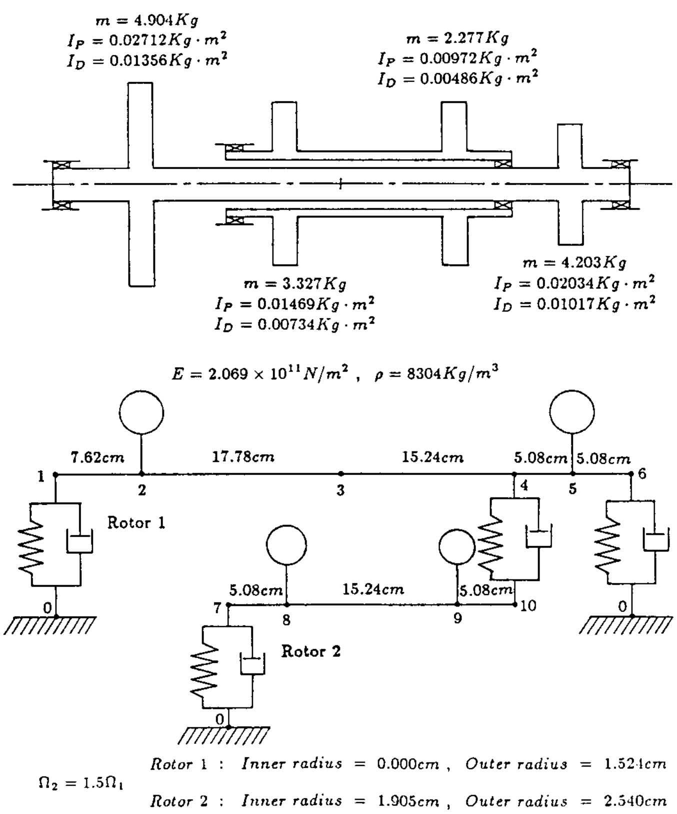

Figure 11 Schematic plot and parameter values of dual rotor system

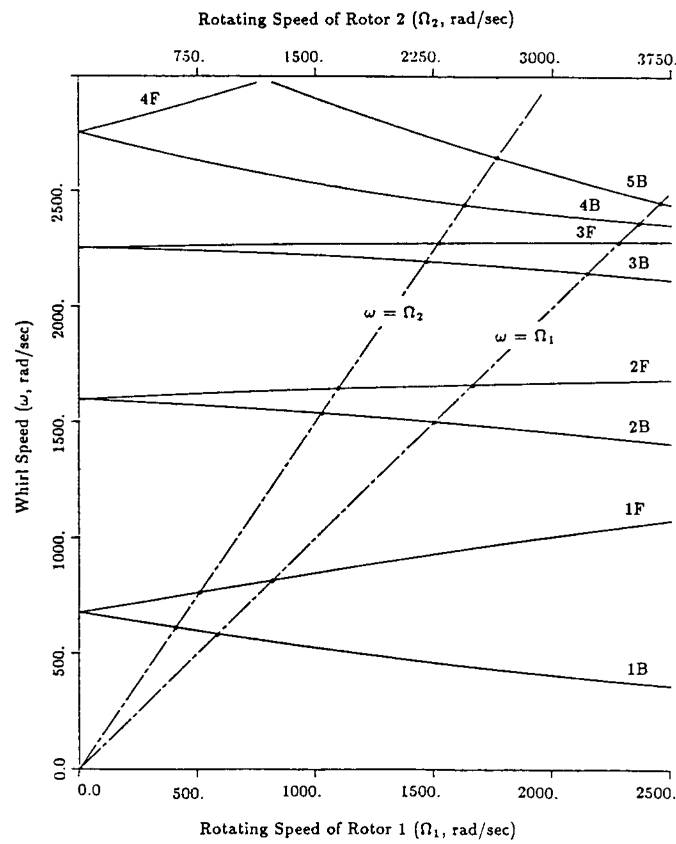

Figure 12 The whipl map using GPEM for dual rotor system

Table 8 Whirl speed results for various levels of modal truncation of dual rotor system for $\Omega_1 = 1500.0$ rad/sec

Mode No.	M_1/M_2=18/12	10/6	6/4	4/2	2/0
$1^{[B;B]}$	460.483	460.587	461.080	461.827	462.478
$2^{[F;F]}$	931.573	931.587	933.814	935.816	938.144
$3^{[B;B]}$	1500.164	1500.557	1501.162	1502.007	1518.437
$4^{[F;F]}$	1657.883	1657.963	1658.332	1661.702	1684.147
$5^{[B;B]}$	2191.757	2192.673	2198.312	2201.122	2252.444
$6^{[F;F]}$	2273.365	2274.252	2292.499	2299.289	2331.544
$7^{[B;B]}$	2453.515	2454.822	2490.747	2501.737	2501.901
$8^{[B;B]}$	2725.233	2729.219	2775.545	2789.907	2894.072
$9^{[F;F]}$	3224.073	3224.318	3232.292	3273.106	3299.574
$10^{[B;B]}$	3354.284	3357.525	3404.565	3573.703	3966.219
$11^{[F;F]}$	4094.309	4094.792	4099.571	4123.738	4577.460
$12^{[F;F]}$	5880.484	5892.795	5921.292	6068.933	6387.456
Frequency Error			< 1.0%	< 7.0%	

(1). Superscripts $[B;F]$ denote that the whirl motion is backward for Rotor 1 and forward for Rotor 2 respectively.

(2). M_1,M_2 : Number of retained constrained normal modes for Rotor 1 and Rotor 2, respectively.

(3). DOF = $M_1 + M_2 + 10$.

(4). Unit of whirl speed is *rad/sec*.

REFERENCES:

Adams, M.L., 1980, "Nonlinear Dynamics of Flexible Multi-Bearing Rotors," Journal of Sound and Vibration, 71(1), pp. 129-144.

Chen, W.J., 1987, "Optimal Design and Parameter Identification of Flexible Rotor-Bearing System." Ph.D. Thesis, Arizona State University.

Childs, D.W., and Graviss, K., 1982, "A Note on Critical-Speed Solutions for Finite-Element-Based Rotor Models," Journal of Mechanical Design, Vol. 104, pp.412-415.

Childs, D.W., 1978, "The Space Shuttle Main Engine High-Pressure Fuel Turbopump Rotor Dynamic Instability Problem." ASME trams., J. of Engineering for Power , Vol. 100, No.1, pp.48-57.

Crandall, S.H., and Yeh, N.A., 1986, "Component Mode Synthesis of Multi-Rotor Systems," Proceedings of the Euromech-Colloquisum 219, Refined Dynamical Theories of Beams, Plates and Shells and Their Applications, pp. 44–55.

Crandall, S.H., and Yeh, N.A., 1989, "Automatic Generation of Component Modes for Rotordynamic Substructures," Journal of Vibration, Acoustics, Stress, and Reliability in Design, Vol. 111, No.1, pp. 6–10.

A.D., 1975, "A General Method for Stability Analysis of Rotating Shafts," Ingenieur-Archieve, Vol. 44, pp. 9-20.

Dimentberg, F.M., 1961, Flexural Vibrations of Rotating Shafts, London: Butterworth.

Eshleman, R.L. and Eubanks, R.A., 1969, "On the Critical Speeds of a Continuous Rotor," Journal of Engineering for Industry, Vol. 91, pp. 1180–1188.

Gasch, R., 1976, "Vibration of Large Turbo-Rotors in Fluid Film Bearings on Elastic Foundation." Journal of Sound and Vibration, 47(1), pp.53-73.

Gladwell, G.M.L. and Bishop, R.E.D., 1959, "The Vibration of Rotating Shafts Supported in Flexible Beaings," Journal of Mechanical Engineering Science Vol. 1, pp. 195–206.

Gu, J. 1986, "An Improved Transfer Matrix-Direct Integration Method for Rotor Dynamics, " Journal of Vibration, Acoustics, Stress, and Reliability in Design, Vol. 108, pp.182-188.

Hwang, J.L., and Shiau, T.N., 1989, "An Application of Generalized Polynomial Expansion Method to Nonlinear Rotor Bearing System," Submitted to ASME, Journal of Vibrations and Acoustics for publication.

IMSL Library, 1984, Mathematical Applications, Inc. Houston, Texas.

Kumar, A.S., and Sankar, T.S., 1986, "A New Transfer Matrix Method for Response Analysis of Large Dynamic Systems," Computers and Structures, Vol.23, No.4, pp. 545-552.

Lee, C.-W. and Jei, Y.-G. 1988, "Modal Analysis of Continuous Rotor-Bearing Systems," Journal of Sound and Vibration, Vol. 126, pp. 345–361.

Lund, J. W., and Orcutt, F.K., 1967, " Calculations and Experiments on the Unbalance Response of a Flexible Rotor in Fluid Film Bearing," ASME Journal of Engineering for Industry, Vol.89, No.4, pp.705-796.

Lund, J.W., 1974a, " Modal Response of a Flexible Rotor in Fluid-Film Bearings, " ASME Journal of Engineering for Industry, Vol. 96, No.2, pp.525-533.

Lund, J.W., 1974b, " Stability and Damped Critical Speeds of a Flexible Rotor in Fluid-Film Bearings, ASME Journal of Engineering for Industry, Vol.96, pp.509- 517.

Myklestad, N.O., 1944 "A New Method of Calculating Natural Modes of Uncoupled Bending Vibration of Airplane Wings and Other Types of Beams," Journal of Aeronautical Sciences, pp. 153–162.

Nelson, H.D., and McVaugh, J.M., 1976, "The Dynamics of Rotor-Bearing Systems Using Finite Elements, " ASME Journal of Engineering for Industry, Vol.98, pp.593- 600.

Nelson, H.D., 1980, "A Finite Rotating Shaft Element Using Timoshenko Beam Theory," ASME Journal of Mechanical Design, Vol.102, pp.793-803.

Prohl, M.A., 1945, "A General Method for Calculating Critical Speeds of Flexible Rotors, "ASME Journal of Applied Mechanics, Vol.12, pp.A-142-A-148.

Rajan, M., Nelson, H.D., and Chen, W.J., 1985, "Parameter Sensitivity in the Dynamics of Rotor-Bearing Systems," ASME Paper No. 85-DET-35.

Ruhl, R.L., and Booker, J.F., 1972, "A Finite Element Model for Distributed Parameters Turborotor Systems," ASME Journal of Engineering for Industry, Vol. 94, pp. 128–132.

Shiau, T.N. and Hwang, Jon-Li, 1989, "A New Approach to the Dynamic Characteristic of Undamped Rotor-Bearing Systems," ASME Journal of Vibration, Acoustics, Stress, and Reliability in Design, Vol. 111, No. 4, pp. 3;6;3m9–385.

Subbiah, R., Kumar, A.S. and Sankar, T.S., 1988, " Transient Dynamic Analysis of Rotors Using the Combined Methodologies of Finite Elements and Transfer Matrix." ASME Trans. J. of Applied Mechanics, Vol. 55, pp.448-452.

APPENDIX A

The components of $N_p \times N_p$ matrices shwon in equation (14) are of the form as follows:

$$M(m,n) = \int_0^\ell \rho(x)A(x)x^{n+m-2}dx + \int_0^\ell (n-1)(m-1)I_D x^{n+m-4}dx + \sum_{i=1}^{N_d}\left[m_i^d(x_i^d)^{n+m-2} + (n-1)(m-1)I_{Di}^d(x_i^d)^{n+m-4}\right] \quad (A-1)$$

$$G(m,n) = \int_0^\ell (n-1)(m-1)I_p x^{n+m-4}dx + \sum_{i=1}^{N_d}\left[(n-1)(m-1)I_{pi}^d(x_i^d)^{n+m-4}\right] \quad (A-2)$$

$$C_{yy}(m,n) = \sum_{j=1}^{N_b} c_{yyj}^b(x_j^b)^{n+m-2} \quad (A-3)$$

$$C_{yz}(m,n) = \sum_{j=1}^{N_b} c_{yzj}^b(x_j^b)^{n+m-2} \quad (A-4)$$

$$C_{zz}(m,n) = \sum_{j=1}^{N_b} c_{zzj}^b(x_j^b)^{n+m-2} \quad (A-5)$$

$$K_s(m,n) = \int_0^\ell (n-1)(n-2)(m-1)(m-2)EIx^{n+m-6}dx \quad (A-6)$$

$$K_{yy}(m,n) = \sum_{j=1}^{N_b} k_{yyj}^b(x_j^b)^{n+m-2} \quad (A-7)$$

$$K_{yz}(m,n) = \sum_{j=1}^{N_b} k_{yzj}^b(x_j^b)^{n+m-2} \quad (A-8)$$

$$K_{zz}(m,n) = \sum_{j=1}^{N_b} k_{zzj}^b(x_j^b)^{n+m-2} \quad (A-9)$$